

Francesconi, M., Baldini, A. M., Ban, S., Benmansour, H., Cattaneo, P. W., Cei, F., ... Yoshida, K. (2023). The trigger system for the MEG II experiment. *Nuclear Instruments and Methods in Physics Research, Section A: Accelerators, Spectrometers, Detectors and Associated Equipment*, 1046, 167736 (4 pp.). <https://doi.org/10.1016/j.nima.2022.167736>

This manuscript version is made available under the CC-BY-NC-ND 4.0 license <http://creativecommons.org/licenses/by-nc-nd/4.0/>

The trigger system for the MEG II experiment

Marco Francesconi^{a,b,*}, Alessandro M. Baldini^b, Sei Ban^h, Hicham Benmansour^{a,b,c}, Paolo W. Cattaneo^c, Fabrizio Cei^{a,b}, Marco Chiappini^b, Gianluigi Chiarello^b, Luca Galli^b, Flavio Gatti^{f,1}, Matteo de Gerone^f, Marco Grassi^b, Ueli Hartmann^c, Toshiyuki Iwamoto^h, Satoru Kobayashi^h, Ayaka Matsushita^h, Fabio Morsani^b, Donato Nicoló^{a,b}, Rina Onda^h, Wataru Ootani^h, Atsushi Oya^h, Angela Papa^{a,b,c}, Stefan Ritt^c, Massimo Rossella^e, Elmar Schmid^c, Giovanni Signorelli^b, Yusuke Uchiyama^h, Antoine Venturini^{a,b}, Bastiano Vitali^{b,d}, Taku Yonemoto^h, Keisuke Yoshida^h

^aDipartimento di Fisica dell'Università di Pisa, Largo B. Pontecorvo 3, 56127 Pisa, Italy

^bIstituto Nazionale di Fisica Nucleare, Sezione Pisa, Largo B. Pontecorvo 3, 56127 Pisa, Italy

^cPaul Scherrer Institut, 5232 Villigen, Switzerland

^dDipartimento di Fisica dell'Università "Sapienza" di Roma, Piazzale A. Moro 2, 00185 Rome, Italy

^eINFN Sezione di Pavia, Via Bassi 6, 27100 Pavia, Italy

^fINFN Sezione di Genova, Via Dodecaneso 33, 16146 Genoa, Italy

^gDipartimento di Fisica, dell'Università di Genova, Via Dodecaneso 33, 16146 Genoa, Italy

^hICEPP, The University of Tokyo, 7-3-1 Hongo, Bunkyo-ku, Tokyo 113-0033, Japan

Abstract

Intending to improve the current sensitivity on $\mu \rightarrow e\gamma$ decay by one order of magnitude, the MEG II experiment at Paul Scherrer Institute completed the integration phase in 2021 with all detectors successfully operated throughout the subsequent beamtime. Earlier in 2021, the WaveDAQ integrated Trigger and Data Acquisition (TDAQ) system, developed for the readout of the experiment, was completely commissioned. Receiving almost 9000 channels from the detectors, the MEG II TDAQ system is the largest WaveDAQ deployment so far, proving the scalability of the overall design, from bench-top setup through various smaller-size experiments. We will describe how MEG II trigger system reduces the $\sim 10^7$ muon decays at the experiment target down to a 10 Hz event rate by exploiting the signal event characteristics at the online level. The trigger system performs the calorimetric reconstruction of the photon shower and then compares the timing and direction with positron candidates within a 600 ns hard latency time. The first release of the online reconstruction, deployed in 2021, achieved a 2.4 % photon energy resolution at the signal energy of 52.8 MeV and a ~ 2 ns coincidence time resolution among the child particles.

Keywords: Trigger, Data Acquisition, TDAQ, Flavour experiments, Intensity frontier

1. Charge Lepton Flavour Violation searches with muons

The non-observation of Flavour Violation among the Charged Leptons (CLFV effects) shaped our knowledge of the Standard Model of particle physics, and highlights a clear difference between charged leptons and the well-known mixing in the quark sector, especially after the observation of oscillation in neutrino flavours. Theoretical models that aim at solving these differences are expected to produce effects in the range observable by modern experiments against a null Standard Model background [1].

Among all the possible searches for CLFV, the ones involving muons are of high interest, as muons are the lightest unstable lepton that can be conspicuously produced and delivered to dedicated experiments, thanks to their long lifetime.

1.1. The $\mu^+ \rightarrow e^+\gamma$ process: signature and backgrounds

Among the CLFV processes involving muons, the $\mu^+ \rightarrow e^+\gamma$ is considered a golden channel because of its clear two-body signature with both the positron and the photon being monochromatic and emitted in opposite directions, in the muon rest frame.

The main sources of backgrounds for a $\mu^+ \rightarrow e^+\gamma$ search are [2]:

*Corresponding author

Email address: marco.francesconi@pi.infn.it (Marco Francesconi)

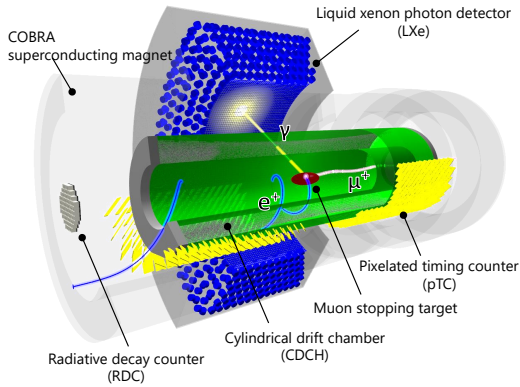


Figure 1: Graphic scheme of the subdetectors of MEG II detector

- The Radiative Muon Decay (RMD), which corresponds to the $\mu^+ \rightarrow e^+ \nu_e \bar{\nu}_\mu \gamma$ process and can mimic the signal if the energy carried by neutrinos is small.
- The accidental coincidence of a positron at signal energy with photons coming from a different source (such as an RMD decay). Due to its accidental nature, this background scales with the second power of the rate of muon decays and therefore becomes dominant when the rate of delivered muons is sufficiently high. However, it can be suppressed with a precise determination of the child particles emission time.

2. The MEG II Experiment

The MEG II Experiment, depicted in Figure 1, was designed [3] around the signal of interest, the $\mu^+ \rightarrow e^+ \gamma$ process. To exploit the clean topology originating from the two-body decay, the world's most intense continuous muon beam, available at Paul Scherrer Institute in Switzerland, is stopped at the centre of the MEG II spectrometer system so that muons decay at rest in experiment frame. The photon detection is accomplished through a Liquid Xenon scintillation detector (LXe) readout by 4092 VUV-sensitive MultiPixel Photon Counters [4] and 686 Photo-Multipliers. The detector provides the measurement of photon energy, conversion position and interaction time while covering $\sim 11\%$ of the solid angle seen from the target and defining the experiment acceptance. Positrons emerging from the target bend in a non-uniform magnetic field which is shaped to select only particles in acceptance with momentum above ~ 40 MeV. Positrons are tracked in a lightweight stereo drift chamber (CDCH) [5] before impinging on one of the two modules of the pixelated Timing Counter detector (pTC) [6], each composed of 256 plastic scintillator counters, whose main goal is to provide the high-resolution timing of the tracks. The Radiative Decay Counter (RDC) is located downstream the target and is made of plastic scintillators and LYSO crystals. It detects low energy positrons which may have been generated by RMD processes.

A common trend in the upgrade from the former MEG Experiment [7] to the new MEG II is an increased segmentation of all detectors to cope with a higher muon stop rate. This is possible also by the extensive use of Silicon PhotoMultipliers (SiPMs) in particular for the LXe, the RDC and the pTC detectors. The high rate of $\approx 10^7 \mu^+ / s$ delivered to the experiment is very important to collect the required statistic to reach a sensitivity of 6×10^{-14} in the planned three years of data collection [8].

Requiring excellent time and charge resolutions despite the harsh pileup environment, detector signals are digitized with 1.4 GHz frequency, so to allow for the complex offline algorithms, to have the complete event picture. However this approach results in an enormous 12 MB uncompressed event size, and therefore a trigger system is crucial to reject the extreme background from the muon beam to a digestible rate while maintaining high efficiency on the signal.

2.1. WaveDAQ: the Trigger and Data Acquisition system

To face the MEG II need for an increased number of channels, a new Trigger and Data Acquisition system [9] named WaveDAQ was designed and commissioned. Such new equipment is capable of accommodating all the required ~ 9000 channels in the same space used by the previous system [10], also including the required amplification and bias stages for the SiPMs.

The heart of the system is the WaveDREAM board (Waveform Domino REAdout Module) which provides a compact 16-channel platform containing two Domino Ring Sampler 4 (DRS4) chips [11]. Those chips are essentially arrays of 1024 sample-and-hold cells that sample and temporarily store the analogue signal from the detector. When a trigger is generated, the actual digitization of the charge in the capacitors is started through an external, slower, Analog to Digital Converter (ADC).

While this provides sampling frequencies at a much higher rate than otherwise possible, it severely constrains the trigger latency to be smaller than the time needed for the chip to sample the input signals 1024 times, that would overwrite the signal pulse which generated the trigger. Operating at a sampling frequency of 1.4 GHz, the maximum allowed trigger latency is 731 ns. In case some pedestal samples are required in front of the pulse the trigger latency has to be further reduced.

The MEG II WaveDAQ is made of 35 custom-made crates each housing 16 WaveDREAM boards plus an additional Data Concentrator Board (DCB), for data streaming to storage, and a Trigger Concentration Board (TCB), for the gathering and the aggregation of trigger information within the crate. Such information is then forwarded to a dedicated crate containing only TCBs where the information is finally aggregated and forwarded to the *Master Trigger Board*, which finally generates the trigger for the whole experiment.

3. The trigger logic

MEG II trigger algorithms must carefully balance the required rate reduction with the hard constraint on trigger latency

coming from DRS4 chips. In particular, this balancing is evident in the decision not to include any information coming from the CDCH detector: the time required for signal formation can indeed reach 150 ns, leaving not enough time to perform any significant processing of the information.

A major contribution to the trigger latency originates from the digitization of the input signals. Needing energy-based triggers for the LXe detector, the WaveDREAM board exploits the same onboard ADC, used to readout the DRS4 chips, to provide also the sampling of signals at 80 MHz for trigger computations.

However not all detectors require the information on the signal amplitude, so an additional leading-edge discriminator is available on all WaveDREAM channels; in this way, the conversion latency of the ADC can be avoided and, at the same time the discriminator output is oversampled at 640 MHz to improve the signal timing.

Another important point in the optimization of trigger latency was the design of the inter-board communication scheme [12]. The pieces of information have indeed to be transmitted three times before they reach the Master Trigger Board, so even spending only 3 clock cycles (that at 80 MHz clock are just 37.5 ns) the total impact on the trigger latency is 112.5 ns, which is of the same order as the ADC conversion time.

The WaveDAQ system supports 64 different triggering lines, that are defined in the firmware to fit the experiment needs; 45 lines are currently being used in MEG II implementation. In addition to the $\mu^+ \rightarrow e^+\gamma$ triggers, that will be described in the next section, part of them are assigned to calibration triggers, such as the pulse shape identification algorithms to select α -particle sources in Xe detector [13].

In the next section, we will focus on describing the $\mu^+ \rightarrow e^+\gamma$ trigger but the WaveDAQ system also performs other trigger selection to fit the experiment calibration purposes. For example, a pulse shape identification algorithm is available [13], to select energy deposits from the α -particle sources in the LXe detector.

3.1. Design of the $\mu^+ \rightarrow e^+\gamma$ trigger

The online selection used for $\mu^+ \rightarrow e^+\gamma$ search is based on the one used for the previous MEG experiment [9]. It can be summarized by the coincidence of three conditions:

- *QSUM Condition*: Energy deposit in the LXe detector.
- *Time Condition*: Time coincidence of a LXe energy deposit and a hit in the pTC.
- *DirectionMatch Condition*: Request that the LXe energy deposit location and the hit in the pTC agree with the topology expected for a signal positron (back-to-back with 52.8 MeV track in the magnetic field).

The selections are implemented in the Field Programmable Gate Array chips available on the WaveDREAM and in the three-layer aggregation tree made out of TCB boards.

In more detail, the QSUM Condition is essentially a threshold on the weighted sum of ADC amplitudes from all scintillation photon detectors in the LXe detector. The channel-

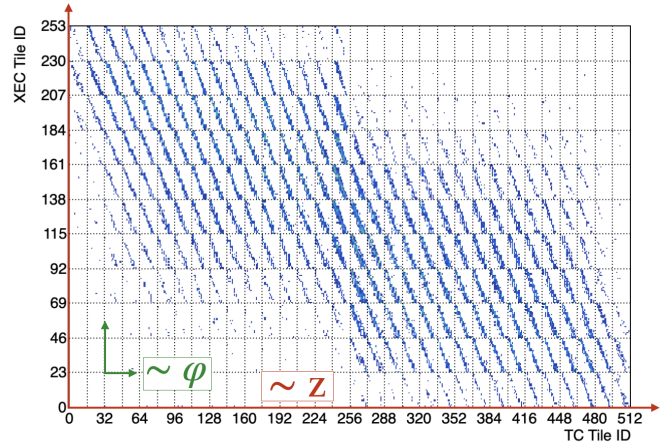


Figure 2: Direction Match Table obtained from signal MonteCarlo simulation. X axis is plastic counter ID on the pTC, Y axis is the conversion positron ID in the LXe. Considering cylindrical coordinates from the MEG II target, both IDs goes first along ϕ direction (in each grid piece) and then along Z through the whole plot.

dependant pedestal value is automatically estimated and removed through an algorithm that computes the running average of the previous pedestal samples. After that, a programmable 8-bit weight is applied to correct for variations of gain, photon detection efficiency and photocathodic coverage.

The Time Condition requires the selection of the conversion point in the LXe, as well as the impact position of the positron in the pTC. The former step is accomplished by selecting the WaveDREAM with the highest number of discriminators above the threshold, and the latter exploits a feature of the pTC detector, where the detector cabling follows the detector segmentation so that the channel with smaller index are placed before the others along the expected positron track. Then the time of the corresponding signal is selected, averaged, and compared.

Finally, the DirectionMatch Condition exploits the two same hit estimations from the LXe and pTC detectors: for a signal event, the back-to-back topology and the monochromatic positron momentum put a constrain on the channel pairs that are possible. To take into account the finite beam spot on the target and the effect of material along the positron path, a full Monte-Carlo simulation of signal events is used and figure 2 shows the pairs which will be enabled in the coincidence.

3.2. The operation in 2021 Physics Run

The complete MEG II detector setup was assembled in early 2021 and commissioned during the first experiment Physics run in fall [14]. This included the full WaveDAQ system, both in hardware and in software, and the first version of the $\mu^+ \rightarrow e^+\gamma$ trigger selection.

In figure 3 the response of the QSUM Condition is shown by two calibration lines obtained by the *Charge Exchange Reaction*, in which a beam of negative pions is stopped in a liquid hydrogen target to produce neutral pions. By selecting the collinear photon pairs we obtained two essentially monochromatic lines of 55.5 MeV and 82.8 MeV, from which we esti-

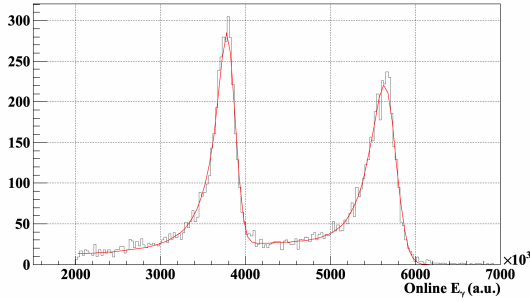


Figure 3: Liquid Xenon detector energy spectrum during Charge Exchange calibration. The two lines are obtained selecting endpoint of π^0 decays by cutting on the opening angle.

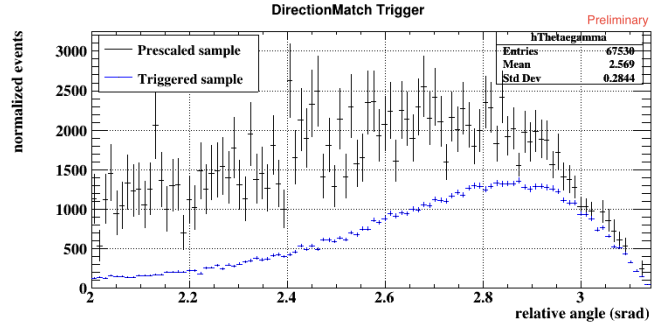


Figure 5: Effect of Direction Match condition on relative angle, there is not enough statistics in the signal region ($> \pi - 20$ msrad to perform the efficiency from the ratio like in Figure 4

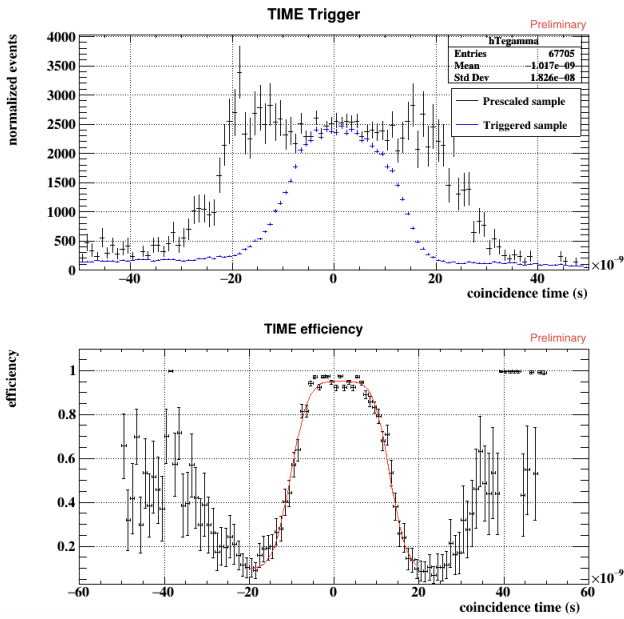


Figure 4: Time condition efficiency and resolution obtained by comparing data from two trigger lines.

mated an online energy resolution of $\sim 2.4\%$ at signal energy.

For what concerns the Time Condition, we can obtain its resolution by comparing the reconstructed distribution of the accidental background for two different thresholds so that no external input is necessary. In particular, we can use a prescaled trigger with wider time cuts to obtain the unbiased distribution in parallel to the one obtained by the main trigger. Figure 4 shows the distribution of the reconstructed time differences for the two triggers and, on the bottom, their ratio. The fit of the two time edges yields an online time resolution of ~ 2 ns.

A similar check is shown in Figure 5 on the reconstructed relative angle. Such plot, differently from the one of figure 4 is highly sensitive to the performance the offline tracking of the positron that, at the moment of writing, was being finalized on 2021 dataset. Therefore only a subset of runs were included in plots of Figure 4 and 5.

4. Conclusions

The 2021 Physics run was the first long operation of the MEG II experiment in its physics data-taking configuration. During the whole period, the WaveDAQ system recorded data correctly and the MEG II trigger was successfully operated with a trigger rate of ~ 10 Hz at $4 \times 10^7 \mu/s$. The 2021 run period will be key to develop and validate both online and offline reconstructions, looking forward to the 2022 long data-taking which will be the first of three years needed for the MEG II experiment to reach the 6×10^{-14} sensitivity goal. Finally, the quality of the dataset was proven by the observation of the Radiative Muon Decay peak which has very close similarities to the $\mu \rightarrow e\gamma$ signal.

References

- [1] L. Calibbi, G. Signorelli, Charged lepton flavor violation: an experimental and theoretical introduction, Riv. Nuovo Cimento 41 (2018) 71–174. arXiv:1709.00294, doi:10.1393/ncr/i2018-10144-0.
- [2] Y. Kuno, Y. Okada, Muon decay and physics beyond the standard model, Rev. Mod. Phys. 73 (1) (2001) 151–202. arXiv:hep-ph/9909265, doi:10.1103/RevModPhys.73.151.
- [3] A. M. Baldini, E. Baracchini, C. Bemporad, et al., The design of the MEG II experiment, Eur. Phys. J. C 78 (5) (2018) 380. doi:10.1140/epjc/s10052-018-5845-6.
- [4] K. Ieki, T. Iwamoto, D. Kaneko, S. Kobayashi, et al., Large-area mppc with enhanced vuv sensitivity for liquid xenon scintillation detector, Nucl. Instrum. Methods A 925 (2019) 148–155. doi:10.1016/j.nima.2019.02.010.
- [5] M. Chiappini, A. M. Baldini, G. Cavoto, et al., Commissioning of the MEG II tracker system, Journal of Instrumentation 15 (06) (2020) C06056–C06056. doi:10.1088/1748-0221/15/06/c06056. URL <https://doi.org/10.1088/1748-0221/15/06/c06056>
- [6] M. Nishimura, F. Berg, M. Biasotti, et al., Full system of positron timing counter in meg ii having time resolution below 40 ps with fast plastic scintillator readout by sipms, Nucl. Instrum. Methods A 958 (2020) 162785. doi:10.1016/j.nima.2019.162785.
- [7] J. Adam, X. Bai, A. M. Baldini, E. Baracchini, et al., The MEG detector for $\mu \rightarrow e\gamma$ decay search, Eur. Phys. J. C 73 (2013) 2365. arXiv:1303.2348, doi:10.1140/epjc/s10052-013-2365-2.
- [8] A. M. Baldini, V. Baranov, M. Biasotti, et al., The search for $\mu \rightarrow e\gamma$ with 10-14 sensitivity: The upgrade of the meg experiment, Symmetry 13 (9) (2021) 1591.
- [9] L. Galli, A. M. Baldini, F. Cei, M. Chiappini, et al., WaveDAQ: An highly integrated trigger and data acquisition system, Nucl. Instrum. Methods A 936 (2019) 399–400. doi:10.1016/j.nima.2018.07.067.
- [10] L. Galli, F. Cei, S. Galeotti, M. C., D. Nicolò, G. Signorelli, M. Grassi, An FPGA-based trigger system for the search of $\mu \rightarrow e\gamma$ decay in

- the MEG experiment, *J. Instrum.* 8 (2013) P01008. doi:10.1088/1748-0221/8/01/P01008.
- [11] S. Ritt, The DRS chip: cheap waveform digitizing in the GHz range, *Nucl. Instrum. Methods A* 518 (1-2) (2004) 470–471. doi:10.1016/j.nima.2003.11.059.
- [12] M. Francesconi, A. Baldini, F. Cei, et al., Low latency serial communication for meg ii trigger system, *Nucl. Instrum. Methods A* 936 (2019) 331–332.
- [13] D. Nicolò, A. M. Baldini, C. Bemporad, et al., Real-time particle identification in liquid xenon, *IEEE Transactions on Nuclear Science* (2021) 1–1doi:10.1109/TNS.2021.3099296.
- [14] M. Chiappini, M. Francesconi, S. Kobayashi, M. Meucci, R. Onda, P. Schwendimann, M. I. Collaboration, Towards a new $\mu \rightarrow e\gamma$ search with the meg ii experiment: From design to commissioning, *Universe* 7 (12) (2021) 466.